



# Assessment of the cryoablation margin using MRI–CT fusion imaging in hepatic malignancies

C. Chen<sup>1</sup>, L.C. Xu<sup>1</sup>, Y. Wang<sup>1</sup>, Y.H. Wang<sup>1</sup>, G.D. Li, H.Z. Huang, B. Wang, W.T. Li\*, X.H. He\*

Department of Interventional Radiology, Fudan University Shanghai Cancer Center, Shanghai, 200032, China

## ARTICLE INFORMATION

### Article history:

Received 17 December 2018

Accepted 22 March 2019

**AIM:** To demonstrate the feasibility of magnetic resonance imaging (MRI)–computed tomography (CT) fusion imaging for the assessment of the ablative margin after cryoablation in hepatic malignancies.

**MATERIALS AND METHODS:** This retrospective study analysed 35 patients with 47 liver tumours treated with CT-guided cryoablation. Fusion images of pre-ablation MRI and intraoperative CT data were created on a workstation. Minimal ablative margin (MAM) assessment was categorised into three groups: (I) MAM <0 mm (tumour protruded through the ablation zone), (II) MAM 0–5 mm, and (III) MAM ≥5 mm. Local tumour progression (LTP) was assessed during follow-up.

**RESULTS:** MRI–CT fusion imaging was successfully achieved in 46 (97.9%) of 47 lesions. LTP was detected in 67.4% (31/46) of cases. Twenty-four (77.4%) of 31 LTPs occurred in the sub-capsular region of the liver. Using fusion images, the MAM was classified as groups I, II, and III in 18, 25, and three tumours, respectively. In group I, LTP was found in 15 (83.3%) of 18 lesions, whereas in group II, LTP was detected in 16 (64%) of 25 lesions. The cumulative LTP rate in group II was significantly lower than that in group I ( $p=0.012$ ).

**CONCLUSION:** Pre-ablation MRI and intraoperative CT fusion imaging is feasible and useful for evaluating the MAM of cryoablation in hepatic malignancies.

© 2019 The Royal College of Radiologists. Published by Elsevier Ltd. All rights reserved.

## Introduction

Thermal ablation techniques for the treatment of unresectable primary and secondary malignant hepatic tumours have been developed in recent years.<sup>1</sup> Cryoablation is a long-known ablation technique, which has potential advantages over radiofrequency ablation (RFA), including

\* Guarantor and correspondent: W. Li and X. He, Department of Interventional Radiology, Fudan University Shanghai Cancer Hospital, no. 270 Dongan Road, Xuhui, Shanghai 200032, China. Tel.: +86021 64175590; fax: +86021 64175590.

E-mail addresses: [wentaoli@fudan.edu.cn](mailto:wentaoli@fudan.edu.cn) (W.T. Li), [hxhdoct@hotmail.com](mailto:hxhdoct@hotmail.com) (X.H. He).

<sup>1</sup> These authors contributed equally to this study.

clear ablation zone,<sup>2,3</sup> activation of anti-tumour immune response,<sup>4</sup> limited ablation spread to adjacent critical structures,<sup>5</sup> and less pain post-cryoablation.<sup>6,7</sup> There is an increasing trend towards performing cryoablation in the setting of hepatic malignancies, where cryoablation has shown impressive results.<sup>7,8</sup>

Various imaging techniques are of great importance in monitoring and assessing the consequences of tumour ablation. For the assessment of the minimal ablative margin (MAM) of RFA, the pre- and post-ablation computed tomography (CT)–magnetic resonance imaging (MRI) images or contrast-enhanced ultrasound (CEUS) images were compared using a side-by-side approach<sup>9–11</sup>; however, these approaches are somewhat subjective and difficult to assess accurately and measure the MAM visually. Recently,

novel fusion imaging techniques have been explored to accurately assess the MAM and ablation efficacy in the treatment of hepatocellular carcinoma (HCC)<sup>12–14</sup>; however, to the authors' knowledge, no prior study has evaluated the treatment effect of cryoablation using fusion images, particularly in the liver. Therefore, the purpose of the present study was to demonstrate the feasibility of pre-ablation MRI and intraoperative CT fusion imaging for the evaluation of the treatment effect of cryoablation of hepatic malignancies.

## Materials and methods

### Clinical data

This was a retrospective study of 66 patients with 79 hepatic tumours who underwent cryoablation between August 2013 and September 2016. Patient data were analysed retrospectively using an institutional departmental database approved by the institutional review board with a waiver for informed consent. All of the cases were histopathologically or clinically confirmed as primary and secondary malignant hepatic tumours. Of the 79 tumours, 32 lesions met the exclusion criteria: lack of contrast-enhanced MRI taken within 1 month before cryoablation ( $n=18$ ) at Fudan University Shanghai Cancer Center, a follow-up period of <6 months after cryoablation ( $n=9$ ) and obvious residual lesions on contrast-enhanced CT or MRI images at 1 month after cryoablation ( $n=5$ ). The remaining 47 tumours in 35 patients were included in the present study. Further details of the inclusion and exclusion criteria are presented in the Electronic [Supplementary Material](#). The 35 cases comprised 21 males and 14 females with a mean age of 49.4 years (range 41–79 years). Six patients had six primary malignant hepatic tumours (five HCCs and one intrahepatic cholangiocarcinoma), and 29 patients had 41 hepatic metastases. Of the 41 hepatic metastases, 19 were metastases from colorectal carcinomas. Twenty-two were metastases from other malignant tumours: five pancreatic neuroendocrine tumours, four breast carcinomas, three gastric carcinomas, two laryngeal carcinomas, one cervical carcinoma, one ovarian carcinoma, one renal cell carcinoma, one oesophageal carcinoma, one pancreatic carcinoma, one lung carcinoma, one chest

wall leiomyosarcoma, and one intra-abdominal synovial sarcoma.

### Study protocol

The protocol included contrast-enhanced MRI within 1 month of cryoablation, the cryoablation procedure itself, fusion imaging procedure using pre-ablation MRI, and intra-operative CT images at the end of cryoablation (cryo-needle still in tumour), assessment of the MAM, follow-up period of at least 6 months, and assessment of LTP.

### MRI examinations

All MRI examinations were performed on a 3 T MRI system (Signa Horizon, GE Medical Systems, Milwaukee, WI, USA) with a phased-array body coil. The main imaging parameters and the order of sequences are shown in [Table 1](#). Gadopentetate dimeglumine (0.1 ml/kg body weight) was injected intravenously at a rate of 2 ml/s, followed by the acquisition of contrast-enhanced images using an axial and coronal liver acceleration volume acquisition (LAVA) sequence.

### Percutaneous cryoablation procedure

Cryoablation was performed under local anaesthesia on an inpatient basis by physicians with >5 years of experience. Before the procedure, 10 mg diazepam was administered by intramuscular injection as basal sedation, supplemented with 5 mg analgesic morphine as required. Patients underwent continuous pulse oximetry and electrocardiography (ECG). The Philips 64-slice spiral CT (120 kV, 250 mA, and 3-mm thickness; Philips Healthcare, Andover, MA, USA) was used for imaging guidance, localisation, and intraoperative real-time monitoring of the ablation procedure in order to avoid injury to surrounding critical structures.

A table-top argon gas-based cryoablation apparatus (Precise Cryoablation System; Galil Medical, Yokneam, Israel) with 17-G cryoprobes was used to perform the procedure. The cryoprobes were placed into the lesion within 1.5 cm of the tumour edge, but with <2 cm intervals between the probes.<sup>15</sup> The number and type of probes used were dependent on the preoperative tumour volume in

**Table 1**

The main parameters of magnetic resonance imaging sequences.

Parameter	Axial T1-weighted imaging	Axial T2-weighted imaging	Axial contrast-enhanced LAVA	Coronal contrast-enhanced LAVA
Sequence	Gradient echo	Fast spin echo	Gradient echo	Gradient echo
Breath-hold	Yes	No	Yes	Yes
Fat saturated	No	Yes	Yes	Yes
TR/TE (ms)	230/2.432	6315.8/86.5	2.588/1.2	3.136/1.512
FOV (mm <sup>2</sup> )	380×380	380×380	370×370	420×420
Matrix	320×160	320×192	260×224	260×192
Thickness/gap (mm)	7/2	7/2	5/0	4/0
Flip angle (°)	85	–	15	11

LAVA, liver acceleration volume acquisition; TR, repetition time; TE, echo time; FOV, field of view.

order to ensure that precise ice balls that encompassed the target tumour were produced. After the cryoprobes had been placed, the cryosurgery system was initiated to begin rapid freezing. A double freeze–thaw cycle (15 minutes/cycle: freeze for 10 minutes and thaw for 5 minutes) was performed according to the standard protocol. An additional cycle was necessary if the ablation zone was not satisfied.

#### *Fusion imaging procedure*

If the ablation was considered to be technically effective on contrast-enhanced CT or MRI images within 1 month after cryoablation, fusion imaging was further performed. One radiologist with 8 years of experience in abdominal radiology and who was blinded to the clinical history and follow-up information of the patient created the fusion images. The series of pre-ablation MRI images in which hepatic tumour was clearly demonstrated was judged and chosen for fusion imaging. Pre-ablation MRI and intraoperative CT images at the end of cryoablation (cryo-needle still in the tumour) were transferred into a workstation (Advantage Workstation Volumeshare 5; GE Healthcare;

Buc, France), and the fusion images of MRI–CT were created using the software provided (Integrated Registration, GE Healthcare; Buc, France; Figs 1–4). At first, automatic image registration was performed by aligning MRI and CT images. Then, in order to enhance the image similarity, fine adjustment using blood vessel, cyst, scar, or hepatic contour as landmarks was performed manually. Landmarks closer to the tumour were preferable as they allowed for more accurate fusion of images.<sup>13</sup> The total time required to fuse images was recorded.

#### *Assessment of the MAM*

Fusion images were interpreted by two abdominal imaging radiologists (8 and 10 years of experience, respectively) together and consensus was obtained by discussion. When they judged that the fusion images were suitable for the measurement of the MAM, which is the shortest distance between the boundaries of a tumour and the ablation zone on axial images, they measured the MAM. According to a reported method of CT fusion imaging,<sup>13,16</sup> MAM assessment was categorised into three groups: (I) MAM <0 mm (tumour protruded through the ablation zone)

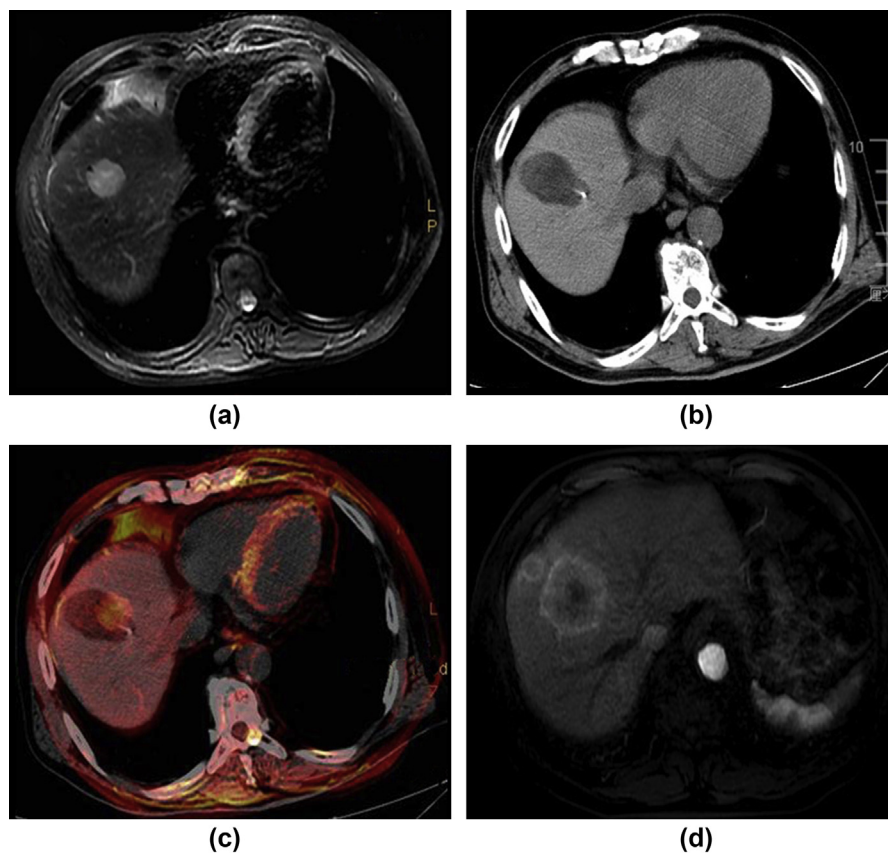


**Figure 1** A 65-year-old man with liver metastases from gastric carcinomas who was treated with percutaneous cryoablation. (a) A single tumour measuring 3.4 cm is clearly visible in segment 8 on the T2-weighted image before cryoablation. (b) The intraoperative CT image at the end of cryoablation (cryo-needle still in the tumour) shows a clear ablation zone. (c) The fusion image is created after automatic rigid registration combined with manual correction. The MAM is categorised as group I: MAM <0 mm (tumour protruded through the ablation zone). (d) Contrast-enhanced MRI image obtained 3 months after cryoablation shows LTP.

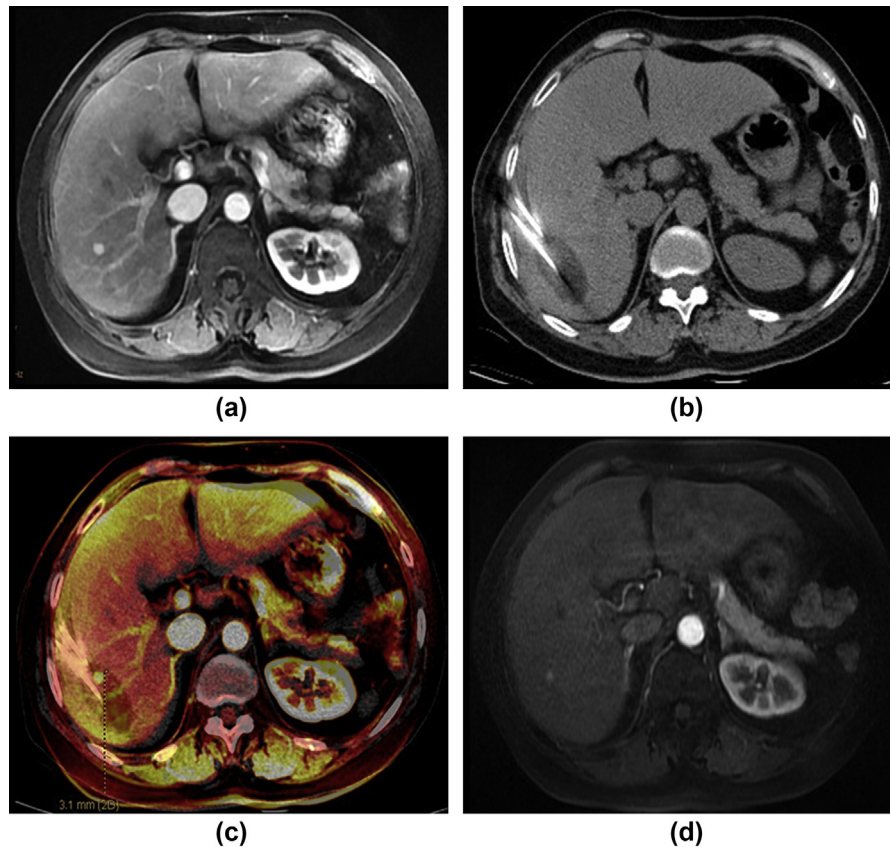


**Figure 2** A 59-year-old man with HCC following radical resection who was treated with percutaneous cryoablation. (a) A single tumour measuring 0.8 cm is noted in segment 5 on the portal phase of contrast-enhanced MRI before cryoablation. (b) The intraoperative CT image at the end of cryoablation shows a clear ablation zone. (c) The fusion image is created after automatic rigid registration combined with manual correction. The MAM is categorised as group II: MAM 0–5 mm. (d) Contrast-enhanced MRI image obtained 4 months after cryoablation shows LTP.

(Fig 1c), (II) MAM 0–5 mm (Figs 2c and 4c), and (III) MAM  $\geq$ 5 mm (Fig 3c).

#### Follow-up procedure

Effectiveness of cryoablation was evaluated by contrast-enhanced CT or MRI within 1 month after ablation. CT examinations were performed with the Somatom Definition AS (Siemens Healthcare, Erlangen, Germany), the Sensation 64 (Siemens Healthcare), and the Brilliance (Philips Healthcare, Best, The Netherlands) using a tube voltage of 120 kV and a current of 250 mA.

If the cryoablation was considered to be technically effective, a follow-up contrast-enhanced CT or MRI examination was obtained every 2–3 months. The presence of LTP was defined as fulfilling at least one of three pre-defined morphological criteria on follow-up CT or MRI images: (1) new tumour nodule within or adjacent to the ablative margin; (2) clear rim of tissue abutting the ablation zone with different attenuation or enhancement than the ablation zone and adjacent normal hepatic parenchyma; and (3) at least 20% increase in the largest diameter of the ablation zone.<sup>17–19</sup>

#### Statistical analysis

Quantitative data were expressed as the mean  $\pm$  standard deviation. The chi-square test was used to compare LTP frequencies between the two groups. The difference in time to LTP between the two groups was assessed using the Mann–Whitney *U*-test. The cumulative LTP rate for each group was calculated using the Kaplan–Meier method, and the statistical significance was analysed using the log-rank test. Comparison was not performed for the difference between group III and the other two groups because of the small size of group III. Statistical analysis was performed using commercially available software (SPSS 20, IBM, Chicago, IL, USA). A *p*-value of  $<0.05$  was considered statistically significant.

#### Results

All patients were treated without severe complications. MRI–CT fusion imaging was achieved successfully in 46 (97.9%) of 47 lesions. Table 2 shows patient clinical characteristics. LTP was detected in 67.4% (31/46) of cases. Further

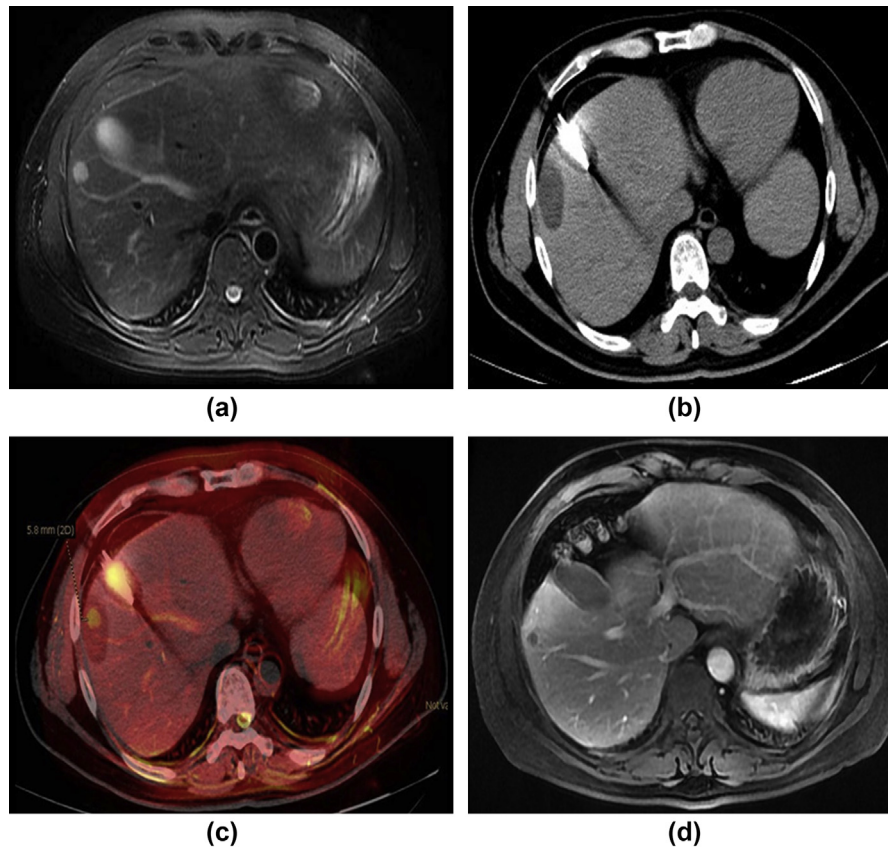


**Figure 3** A 42-year-old man with visible liver metastases from colorectal carcinoma who was treated with percutaneous cryoablation. (a) A tumour measuring 1.2 cm is clearly visible in segment 5 on the T2-weighted image before cryoablation. (b) The intraoperative CT image at the end of cryoablation (cryo-needle still in the tumour) shows a clear ablation zone. (c) The fusion image is created after automatic rigid registration combined with manual correction. The MAM is categorised as group III: MAM  $\geq$  5 mm. (d) The contrast-enhanced MRI image obtained after 9.5 months shows no LTP.

details of the date of cryoablation and LTP are presented in the Electronic [Supplementary Material](#). Twenty-four (77.4%) of 31 LTPs occurred in the subcapsular region of the liver.

#### Fused image creation and MAM

The total time required to fuse images was  $14.57 \pm 1.64$  minutes (range: 10.08–16.52 minutes) in all cases. Using fused images, the MAM was classified as group I, II, and III in 18, 25, and three tumours, respectively ([Table 2](#)).

#### Relationship between MAM and LTP

The frequency of LTP in group I (83.3%; 15/18; [Fig 1](#)) was higher than that in group II (64%; 16/25; [Figs 2 and 4](#)), but there was no significant difference ( $p=0.191$ ). No LTP was found in group III ([Fig 3](#)). The cumulative LTP rate (40%, 56%, and 64% at 1, 2, and 3 years, respectively) in group II ( $n=25$ ) was significantly lower than those (77.8%, 83.3% and 83.3% at 1, 2, and 3 years, respectively) in group I ( $n=18$ ;  $p=0.012$ ; [Fig 5](#)). The cumulative LTP rate of group III was 0% at 1, 2, and 3 years ( $n=25$ ). There was a significant difference in the time to LTP between groups I and II (2–19 months; median, 3 months versus 2–30 months; median, 6 months,  $p=0.037$ ).

## Discussion

The results of the present study support the feasibility of MRI–CT fusion imaging for the assessment of the ablative margin after cryoablation in hepatic malignancies based on several features. First, the total time required to fuse images was  $14.57 \pm 1.64$  minutes (range: 10.08–16.52 minutes). This observation is consistent with other reports in which the total time required to fuse images was  $15.5 \pm 5.5$  minutes (range: 8–22 minutes) in all cases in Wang *et al.*<sup>14</sup> and 15 minutes in all cases in Makino *et al.*<sup>13</sup> Second, a high success rate (97.9%) was obtained for MRI–CT image fusion, which is similar to those shown in previous studies of fusion imaging.<sup>14,20,21</sup> Third, the image quality of the MRI–CT fusion imaging was sufficient for further evaluation. The series in which hepatic tumour in the pre-MRI and ablation zone at intraoperative CT was clearly demonstrated was chosen as images for the fusion imaging. Therefore, the MAM can be clearly observed. These results suggest the feasibility for routine clinical practice.

When the tumour is located in the subcapsular region of the liver, cryoablation has its own potential advantages over RFA.<sup>22–24</sup> Several factors, including freezing temperature, freezing time, thawing, and the number of freeze–thaw

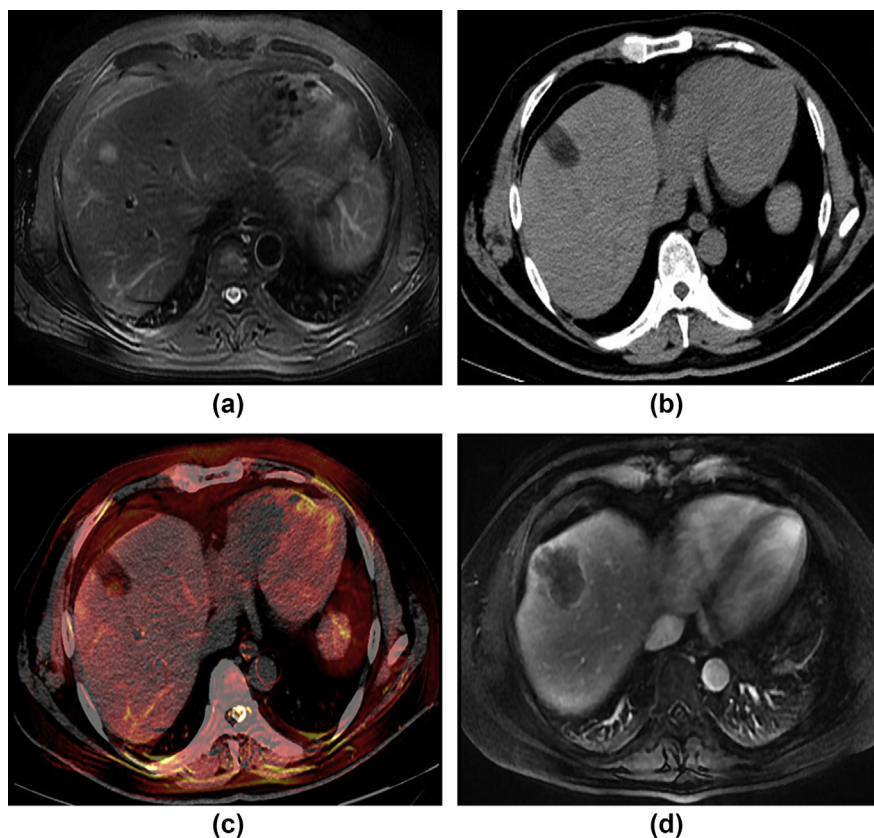


**Figure 4** Same patient as in Fig 3. (a) A tumour measuring 1.5 cm is clearly visible in segment 8 on the T2-weighted image before cryoablation. (b) The intraoperative CT image at the end of cryoablation (cryo-needle still in the tumour) shows a clear ablation zone. (c) The fusion image is created after automatic rigid registration combined with manual correction. The MAM is categorised as group II: MAM 0–5 mm. (d) The contrast-enhanced MRI image obtained after 9.5 months shows LTP.

**Table 2**

Characteristics of cryoablation treated tumours.

	All treated tumours	Treated tumours with LTP	Treated tumours without LTP
Tumours (no.)	46	31	15
Tumours size (cm, mean±SD)	2.70±1.51	2.84±1.70	2.42±1.03
Tumours in the subcapsular region (no.)	32	24	8
Liver segment (no.)			
S1/2/3/4/5/6/7/8	0/1/3/2/7/14/10/9	0/1/2/2/2/10/6/8	0/0/1/0/5/4/4/1
MAM (no.)			
I	18	15	3
II	25	16	9
III	3	0	3

LTP local tumour progression, SD standard deviation, MAM minimal ablative margin.

cycles, influence how effective cryoablation is. In order to form the ideal-sized ice ball, the freezing time increases until a dynamic balance of cold/heat exchange is achieved. The cryoablation procedure can be monitored accurately to ensure complete ablation<sup>7</sup> by virtue of the clear ablation zone on unenhanced CT.<sup>25</sup> In the present study, 32 (69.5%) of 46 treated tumours were located in the subcapsular region of the liver. Nevertheless, 24 (77.4%) of 31 LTPs occurred in the subcapsular region of the liver. For tumours in the subcapsular region in the present study, the freezing time was tightly controlled in order to avoid complications. The results of the study therefore suggest that LTP

occurrence in the subcapsular region of the liver may be the result of incomplete cryoablation. There is increasing clinical and experimental evidence that RFA may, in fact, promote off-target tumorigenic effects in incompletely treated tumours of the ablative margins.<sup>26</sup> Therefore, it is conceivable that incomplete cryoablation may induce such off-target tumorigenic effects, resulting in more LTPs; however, further studies are required to test this hypothesis.

In some studies of CT or MRI fusion imaging, the cumulative LTP rates were clearly stratified by the MAM.<sup>13,27,28</sup> Although a similar MAM classification system was used, the present study is the first to investigate the feasibility of

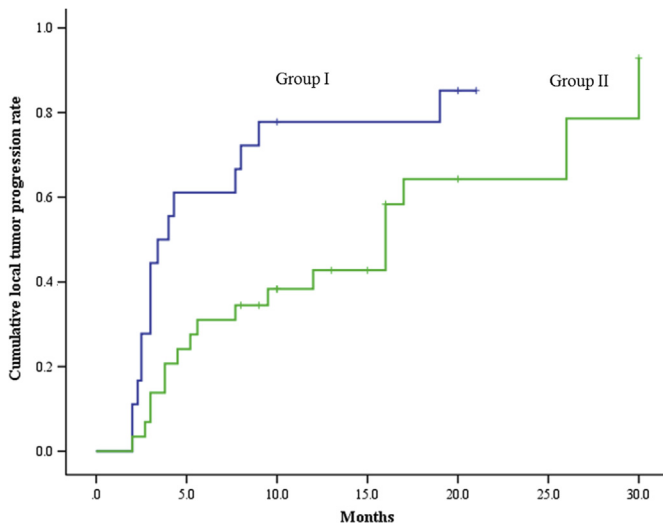


**Figure 5** Cumulative local tumour progression rates in group I and II. The cumulative LTP rate of group I was significantly higher than that of group II ( $p=0.012$ ).

MRI–CT fusion imaging for the assessment of treatment efficacy of cryoablation. The present study demonstrated that 15 of 18 tumours in group I and 16 of 25 tumours in group II developed LTPs, which differs from Koda *et al.*, in which five LTPs were detected in 32 ablative margin (AM) (ablation margin) zero tumours.<sup>28</sup> This difference may be attributed to differences in tumour location or pathological differences in hepatic tumours. Importantly, the cumulative LTP rate in group II was significantly lower than that in group I, which is consistent with previous studies.<sup>13,28</sup> It is possible that tumours that do or do not protrude from the ablation zone eventually progress owing to incomplete ablation. From these results, tumours assessed as group I or group II on MRI–CT fusion images should be re-treated with additional cryoablation to obtain sufficient ablative margin. Additionally, the finding that LTP was not detected in group III is in line with studies reported by Koda *et al.* and Wang *et al.*<sup>14,28</sup> Koda *et al.* demonstrated that AM (+) on MRI with gadolinium-ethoxybenzyl-diethylenetriamine pentaacetic acid (Gd-EOB-DTPA) is adequate to control local progression of HCCs <3 cm.<sup>28</sup> In the present study, only three tumours were classified as a group III MAM.

There were a number of limitations to the present study. First, this is a retrospective study with higher LTP, thereby resulting in limited clinical practice of cryoablation, especially for tumours in the subcapsular region of the liver. Second, in order to achieve complete cryoablation of tumour tissue, the edge of the ice ball must exceed that of the tumour by 1 cm<sup>7,29</sup>; however, in this retrospective study, 18 tumours in group I and 25 tumours in group II had the MAM of <5 mm, which may increase the incidence of LTP. Third, for pre- and post-treatment fusion imaging, there is the challenge of liver deformation because of changes to the patient's position. MRI–CT image fusion was not achieved in one case in this study due to significant deformation of the liver.

In conclusion, the MAM measurement using MRI–CT fusion images is significantly related to LTP. Intraoperative fusion imaging is feasible for the assessment of CT-guided cryoablation efficacy and enables intraoperative treatment evaluation without the need to perform immediate post-contrast-enhanced CT in hepatic malignancies.

## Conflict of interest

The authors declare no conflict of interest.

## Acknowledgements

Tianyou Wang of GE Healthcare, China, kindly provided good advice regarding operation of the workstation. This work was supported by National Key Research and Development Program of China (no. 2016YFC0106203) and Program of Shanghai Hospital Development Center (no. SHDC22017102).

## Appendix A. Supplementary data

Supplementary data to this article can be found online at <https://doi.org/10.1016/j.crad.2019.03.021>.

## References

- Jansen MC, van Hillegersberg R, Chamuleau RA, *et al.* Outcome of regional and local ablative therapies for hepatocellular carcinoma: a collective review. *Eur J Surg Oncol* 2005;**31**(4):331–47.
- Littrup PJ, Ahmed A, Aoun HD, *et al.* CT-guided percutaneous cryotherapy of renal masses. *J Vasc Interv Radiol* 2007;**18**(3):383–92.
- Littrup PJ, Freeman-Gibb L, Andea A, *et al.* Cryotherapy for breast fibroadenomas. *Radiology* 2005;**234**(1):63–72.
- Sabel MS. Cryo-immunology: a review of the literature and proposed mechanisms for stimulatory versus suppressive immune responses. *Cryobiology* 2009;**58**(1):1–11.
- Ladd AP, Rescorla FJ, Baust JG, *et al.* Cryosurgical effects on growing vessels. *Am Surg* 1999;**65**(7):677–82.
- Arciero CA, Sigurdson ER. Liver-directed therapies for patients with primary liver cancer and hepatic metastases. *Curr Treat Options Oncol* 2006;**7**(5):399–409.
- Niu LZ, Li JL, Xu KC. Percutaneous cryoablation for liver cancer. *J Clin Translat Hepatol* 2014;**2**(3):182–8.
- Ng KM, Chua TC, Saxena A, *et al.* Two decades of experience with hepatic cryotherapy for advanced colorectal metastases. *Ann Surg Oncol* 2012;**19**(4):1276–83.
- Goldberg SN, Grassi CJ, Cardella JF, *et al.* Image-guided tumour ablation: standardization of terminology and reporting criteria. *Radiology* 2005;**235**(3):728–39.
- Rhim H, Goldberg SN, Dodd 3rd GD, *et al.* Essential techniques for successful radio-frequency thermal ablation of malignant hepatic tumours. *RadioGraphics* 2001. 21 Spec No:S17–35; discussion S36–19.
- Curley SA. Radiofrequency ablation of malignant liver tumours. *Ann Surg Oncol* 2003;**10**(4):338–47.
- Ahn SJ, Lee JM, Lee DH, *et al.* Real-time US-CT/MR fusion imaging for percutaneous radiofrequency ablation of hepatocellular carcinoma. *J Hepatol* 2017;**66**(2):347–54.
- Makino Y, Imai Y, Igura T, *et al.* Utility of computed tomography fusion imaging for the evaluation of the ablative margin of radiofrequency ablation for hepatocellular carcinoma and the correlation to local tumour progression. *Hepatol Res* 2013;**43**(9):950–8.

14. Wang XL, Li K, Su ZZ, et al. Assessment of radiofrequency ablation margin by MRI-MRI image fusion in hepatocellular carcinoma. *World J Gastroenterol* 2015;**21**(17):5345–51.
15. Wang H, Littrup PJ, Duan Y, et al. Thoracic masses treated with percutaneous cryotherapy: initial experience with more than 200 procedures. *Radiology* 2005;**235**(1):289–98.
16. Makino Y, Imai Y, Igura T, et al. Feasibility of extracted-overlay fusion imaging for intraoperative treatment evaluation of radiofrequency ablation for hepatocellular carcinoma. *Liver Cancer* 2016;**5**(4):269–79.
17. Chopra S, Dodd 3rd GD, Chintapalli KN, et al. Tumour recurrence after radiofrequency thermal ablation of hepatic tumours: spectrum of findings on dual-phase contrast-enhanced CT. *AJR Am J Roentgenol* 2001;**177**(2):381–7.
18. Therasse P, Arbuck SG, Eisenhauer EA, et al. New guidelines to evaluate the response to treatment in solid tumours. European organization for Research and treatment of cancer, national cancer institute of the United States, national cancer institute of Canada. *J Natl Cancer Inst* 2000;**92**(3):205–16.
19. Frich L, Hagen G, Brabrand K, et al. Local tumour progression after radiofrequency ablation of colorectal liver metastases: evaluation of ablative margin and three-dimensional volumetric analysis. *J Vasc Interv Radiol* 2007;**18**(9):1134–40.
20. Kim YS, Lee WJ, Rhim H, et al. The minimal ablative margin of radiofrequency ablation of hepatocellular carcinoma (>2 and <5 cm) needed to prevent local tumour progression: 3D quantitative assessment using CT image fusion. *AJR Am J Roentgenol* 2010;**195**(3):758–65.
21. Fujioka C, Horiguchi J, Ishifuro M, et al. A feasibility study: evaluation of radiofrequency ablation therapy to hepatocellular carcinoma using image registration of preoperative and postoperative CT. *Acad Radiol* 2006;**13**(8):986–94.
22. Silverman SG, Tuncali K, Adams DF, et al. MR imaging-guided percutaneous cryotherapy of liver tumours: initial experience. *Radiology* 2000;**217**(3):657–64.
23. Tatli S, Acar M, Tuncali K, et al. Percutaneous cryoablation techniques and clinical applications. *Diagn Interv Radiol* 2010;**16**(1):90–5.
24. Wu S, Hou J, Ding Y, et al. Cryoablation versus radiofrequency ablation for hepatic malignancies: a systematic review and literature-based analysis. *Medicine* 2015;**94**(49):e2252.
25. Lee Jr FT, Chosy SG, Littrup PJ, et al. CT-monitored percutaneous cryoablation in a pig liver model: pilot study. *Radiology* 1999;**211**(3):687–92.
26. Ahmed M, Kumar G, Moussa M, et al. Hepatic radiofrequency ablation-induced stimulation of distant tumour growth is suppressed by c-Met inhibition. *Radiology* 2016;**279**(1):103–17.
27. Makino Y, Imai Y, Igura T, et al. Comparative evaluation of three-dimensional Gd-EOB-DTPA-enhanced MR fusion imaging with CT fusion imaging in the assessment of treatment effect of radiofrequency ablation of hepatocellular carcinoma. *Abdom Imaging* 2015;**40**(1):102–11.
28. Koda M, Tokunaga S, Okamoto T, et al. Clinical usefulness of the ablative margin assessed by magnetic resonance imaging with Gd-EOB-DTPA for radiofrequency ablation of hepatocellular carcinoma. *J Hepatol* 2015;**63**(6):1360–7.
29. Hinshaw JL, Lee Jr FT. Cryoablation for liver cancer. *Tech Vasc Interv Radiol* 2007;**10**(1):47–57.